Identification of Differential Genes by Microarray and COL6A1 Induced the Bone Metastasis of Non-Small Cell Lung Cancer

Nan Li
Hebei Medical University Third Affiliated Hospital
Xiaohui Cao
Heibei Medical University Third Affiliated Hospital
Wei Li
Hebei Medical University Third Affiliated Hospital
Yunfang Li
Hebei Medical University Third Affiliated Hospital
Zongmao Zhao (zzm692017@sina.com)
Second Hospital of Hebei Medical University
Ming Liu
Hebei Medical University Third Affiliated Hospital

Research article

Keywords: Non-small cell lung cancer, bone metastasis, gene microarray, collagen family collagen 6A1

Posted Date: December 1st, 2020

DOI: https://doi.org/10.21203/rs.3.rs-113918/v1

Abstract

Background: Non-small cell lung cancer (NSCLC) is a major cause of cancer-related death worldwide with bone metastasis as the most prevalent events in advanced cancer patients. However, its pathogenesis has not been clearly described.

Methods: In the present study, differentially expressed genes (DEGs) were filtered through gene expression microarray between NSCLC tissue samples with or without bone metastasis. Subsequently, collagen family collagen 6A1 (COL6A1) was chosen as the target gene through Ingenuity Pathway Analysis and qRT-PCR validation of the 8 Top genes. And we evaluated the osteogenic capacity of HOB and hES-MP 002.5 cells through RT-qPCR, Western blot, Alizarin Red Staining and ALP staining.

Results: A total of 364 DEGs including 140 up-regulated genes and 224 down-regulated genes were identified in NSCLC tissues with bone metastasis. GO analysis indicated that the upregulated and downregulated genes were mainly enriched in cellular process, metabolic process and biological regulation. KEGG pathway analysis revealed that the upregulated genes were mainly concentrated in cysteine and methionine metabolism, oxidative phosphorylation, and ribosome; the downregulated genes were mainly concentrated in the transcriptional misregulation in cancer, ribosome, and mitophagy-animal. Besides, the results of RT-qPCR, western blot and immunohistochemistry proved that COL6A1 was highly expressed in NSCLC tissue samples with bone metastasis. And we revealed that HOB and hES-MP 002.5 cells have osteogenic capacity through RT-qPCR, Western blot, Alizarin Red Staining and ALP staining . Moreover, the results of cell adhesion assay also proved that high expression of COL6A1 in HARA-B cells can induce its adhesion ability on osteoblasts, and low expression of COL6A1 in HARA-B cells can reduce its adhesion ability on osteoblasts.

Conclusions: Therefore, our data revealed that the COL6A1 might represent a diagnostic marker or therapeutic target for bone metastasis in NSCLC.

Background

Non-small cell lung cancer (NSCLC), which is one of common causes of cancer-related deaths, affects about 1.5 million people every year in the world wide(1, 2). Although its occurrence is high in economically developed countries, the incidence and mortality of NSCLC is also found be increased recently in developing countries such as China(3). Despite much progress on different treatment measures has been made, the 5-year survival rate is less than 30%, still representing a pressing challenge on health problem(4). The poor prognosis for NSCLC is generally due to the inability of treating during the advanced stages, in which metastases often occurs(5). Notably, bone is the most preferred site of metastases from NSCLC because of its abundant blood flow and highly expressed adhesion molecules on tumor cells(6, 7). Clinically, bone metastases are often manifested by patients with malignant tumors and it is reported that 14–40% advanced NSCLC patients will develop bone metastases(5, 8, 9). Furthermore, bone metastasis in NSCLC patients will lead to skeleton-associated morbidity, such as

extremely debilitating pain, fracture and spinal compression, resulting in a shorter survival of time and a worse prognosis(10). Hence, the early detection of bone metastasis is critical for a better clinical management for advanced NSCLC patients.

NSCLC with bone metastasis is a multifaceted biological process in which several genes and signaling pathways are involved. Thus, elucidating the key role of these genes and signaling pathways involved in the regulation of NSCLC bone metastasis are critical for finding new diagnostic markers or therapeutic targets. With the advances in bioinformatics in recent years, many new approaches have been used for disease therapy and diagnosis. Microarray analysis has increasingly become a promising tool for characterizing the molecular mechanisms of many types of cancers(11). Moreover, gene expression profiles combined with bioinformatics analysis have also been used to reveal the underlying molecular mechanisms associated with NSCLC development(12, 13).

In the present study, we utilized high-throughput transcriptome expression microarray analysis technology to identify differential expression genes (DEGs) between NSCLC tissue samples with and without bone metastasis. Furthermore, enriched functional categories were applied to reveal the altered signaling pathways between the two groups. Finally, we examined the expression level of collagen 6A1 (COL6A1) at the mRNA and protein level, providing evidence for the use of COL6A1 as potential diagnostic marker or therapeutic target for NSCLC patients with bone metastasis.

Methods

Patients and sample collection

A total of forty patients with lung squamous cell carcinoma were included in the Third Hospital of Hebei Medical University during February 2019 through September 2019, none of the patients had received radiotherapy or chemotherapy before surgery. Samples were immediately frozen in liquid nitrogen and then stored at -80 °C until further use. The study protocol had been approved by the ethics committee of the Third Hospital of Hebei Medical University. All patients have signed the informed written consents.

RNA extraction and purification

Total RNA was extracted and purified using RNeasy mini kit (Cat. No.74106, QIAGEN, GmBH, Germany) following the manufacturer's instructions, and checked for an RNA integrity number (RIN) to inspect the RNA integration by an Agilent Bioanalyzer 2100 (Agilent technologies, Santa Clara, CA, US). RNA samples having a RIN value of 7.0 or 28s/18s≥0.7 indicated that qualified.

RNA amplification and labeling

Total RNA was amplified and labeled by using Low Input Quick Amp Labeling Kit, One-Color (Cat. No. 5190-2305, Agilent technologies, Santa Clara, CA, US) following the manufacturer's instructions. Labeled cRNA were purified by RNeasy mini kit (Cat. No. 74106, QIAGEN, GmBH, Germany).

Microarray hybridization analysis

Each slide of labeled cDNA was hybridized with 1.65 μg Cy3-labeled cRNA using Gene Expression Hybridization Kit (Cat. No. 5188-5242, Agilent technologies, Santa Clara, CA, US) in Hybridization Oven (Cat. No. G2545A, Agilent technologies, Santa Clara, CA, US). After 17 hours hybridization, slides were washed in staining dishes (Cat. No. 121, Thermo Shandon, Waltham, MA, US) with Gene Expression Wash Buffer Kit (Cat. No. 5188-5327, Agilent technologies, Santa Clara, CA, US).

Signal collection and data acquisition

Slides were scanned by Agilent Microarray Scanner (Cat. No. G2565CA, Agilent technologies, Santa Clara, CA, US) with default settings, Dye channel: Green, Scan resolution=3μm, PMT 100%, 20bit. Data were extracted with Feature Extraction software 10.7 (Agilent technologies, Santa Clara, CA, US). Raw data were normalized by Quantile algorithm, limma packages in R. All procedures were carried out according to the standard protocols.

Data analysis

Raw data were subjected to quality control, pre-processing and GC-RMA normalization Hierarchical clustering analysis was used to categorize the data into two groups of different expression patterns. Statistical analysis of genes was performed by paired t-test and the calculation of log2-fold change (log FC). DEGs were identified with the cut-off criteria of false discovery rate (FDR)-corrected P value < 0.05 and |log2 fold-change (FC)| > 2 (Benjamini and Hochberg method). Functional groups and biological pathway enrichment analyses for the common DEGs were performed using the Database for Gene Ontology (GO) functional and Kyoto Encyclopedia of Genesand Genomes (KEGG)(14).

IPA functional analysis

DEGs were functionally analyzed based on the Ingenuity Pathway Analysis (IPA) software, which is based on computational algorithms that analyze the functional connectivity of the genes from information obtained within the IPA database. Canonical pathway analysis was performed using IPA. The created genetic networks describe functional relationships among genes or proteins based on known associations from the database. Networks were ranked according to their biological relevance to the gene list provided. The *p* value calculated by Fisher's exact test was used to determine the probability of the association not due to chance alone.

Quantitative RT-PCR analyses

Verify gene expression changes measured by microarray analysis. Total RNA from pulmonary tumor tissue samples with and without bone metastases were isolated by using TRIZOL reagent (Invitrogen, USA). The quantity and purity of RNA was assessed by absorbance at 260 nm and 280 nm. 1μg of total RNA was used as template for cDNA synthesis using the Reverse Transcription System kit (TaKaRa Bio, Shiga, Japan). Real-time PCR reactions were performed with DNA Master SYBR Green. Average Ct values

from triplicate analyses were normalized from average Ct values of GAPDH. All primer sequences were displayed in Table 1.

Table 1.

Specific primers for Quantitative RT-PCR analyses

ID	Sequence(5’- 3’)	Product Length(bp)
For internal reference		
GAPDH.F	TGTTCGTCATGGGTGTGAAC	154
GAPDH.R	ATGGCATGGACTGTGGTCAT	
For Osteogenic ability detection		
ALP.F	ACTGGGGCCTGAGATACCC	185
ALP.R	TCGTGTTGCACTGGTTAAAGC	
RUNX2.F	TGGTTACTGTCATGGCGGGTA	101
RUNX2.R	TCTCAGATCGTTGAACCTTGCTA	
For microarray DEGs verification		
COA3 F	CTGGATTCTAAGCGTGGAGAG	236
COA3 R	AGCTCATCTAGGAAACGCTC	
APPL1 F	GACAGCCCGCAGACAAG	136
APPL1 R	GGTGTGTTGCTGCACTTAAT	
COL6A1 F	ACACCGACTGCGCTATCAAG	90
COL6A1 R	CGGTCACCACAATCAGGTACTT	
TERF1 F	ACAGCGCAGAGGCTATTATTC	121
TERF1 R	TCAAACTGTGCATCAAGGGT	
TST F	TATCAGTGCTCAATGGTGGC	104
TST R	GTCCAGTGTGGCTTTGAAGA	
CD133 F	AAACCTGCAACAGCATCAGA	150
CD133 R	GGGATTGATAGCCCTGTTGG	
RALY F	CCCAAGTCCATCAACTCTCG	268
RALY R	CTGCTCTCTTTAGCCCCTTG	
Prominin2 F	CTCCGTGAAGGTGAATGAGG	159
Prominin2 R	TTGTGCTCTGTCTTCACTCG	

Western blotting

Total protein was extracted from tissue samples by using RIPA buffer. Protein concentration was determined by Bradford protein assay. Total protein was separated bysodium dodecyl sulfate polyacrylamide gel electrophoresis (SDS-PAGE) prior to transferring onto a PDVF membrane (Millipore, Bedford, MA, USA). Blocking was performed for 1 h with 4% milk at room temperature for 1.5 h and membranes were subsequently incubated at 4˚C overnight with anti-COL6A1 (1:500 dilution; Abcam, cat. no. ab151422), anti-ALP (1:1000 dilution; Abcam, cat. no. ab83259) and anti-RUNX2 (1:1000 dilution; Abcam, cat. no. ab23981). Goat anti-Mouse IgG H&L (HRP) (1:2000 dilution; Abcam, cat. no. ab6721) was then applied at room temperature for 2h before detection using enhanced chemiluminescence (ECL) substrate (Beyotime Biotechnology, China). GAPDH protein was used as loading control for normalization. The quantitative results were calculated by the ImageJ software (version 1.50b; National Institutes of Health, Bethesda, MD).

Immunohistochemistry (IHC) assay

Surgically pulmonary tumor tissue samples (with and without bone metastasis) were fixed in 4% paraformaldehyde and embedded in paraffin. Sectioned tissue samples were dehydrated with xylene and ethanol, and incubated in sodium sulphate buffer (pH = 6.0) at 100 °C. After washing samples with PBS, anti-COL6A1 (1:100 dilution; Abcam, cat. no. ab151422) was added and incubated at 4 °C overnight. Goat anti-Mouse IgG H&L (HRP) (11000 dilution; Abcam, cat. no. ab6721) was added and incubated for 30 min at 37 °C. After the DAB staining, the slides were then counterstained with hematoxylin for observation under regular microscopy.

Cell culture and osteogenic induction

HOB, hES-MP 002.5 and M-7 cells were obtained from the ATCC, and maintained in DMEM/HIGH medium (Hyclone) with 10% fetal bovine serum (FBS, Hyclone). All cells were incubated at 37˚C and 5% CO2. HOB, hES-MP 002.5 and M-7 cells were induced using osteoblast inducing conditional media (PUHE Biomedical, Cat. no. CTCC Y001) for 14 days.

Alizarin Red Staining

1×10^3 cells/well HOB, hES-MP 002.5 and M-7 cells were cultured in 96-well paltes, perspectively. After osteogenic induction for 14 days, Alizarin Red Staining was conducted using the kit (PUHE Biomedical, Cat. No. CTCC JD001) according to the manufacturer’s instructions.

ALP staining

1×10^3 cells/well HOB, hES-MP 002.5 and M-7 cells were cultured in 96-well paltes, perspectively. After osteogenic induction for 14 days, ALP staining was conducted using the kit (PUHE Biomedical, Cat. No. CTCC JD002) according to the manufacturer’s instructions.

Cell adhesion assay

As described in previous study(15), HOB, hES-MP 002.5 and M-7 cells were grown into 6-well paltes. 1×10^3 HARA-B cells, which were stable expression of COL6A1 (GFP from the COL6A1 overexpressed plasmid or shRNAs)were co-cultured with HOB, hES-MP 002.5 and M-7 cells for 30 min at 37°C, perspectively. And the treated HARA-B cells ($1x10^3$ cells/well) were overlaid directly in a dish and incubated for 30 min at 37°C and 5% CO_2. The cells were washed in PBS and fixed with 4% paraformaldehyde. The adhered GFP-expressing cells were observed and counted under the fluorescence microscope.

Statistical analysis

Statistics were performed using GraphPad Prism (GraphPad Software Inc, San Diego, CA, USA) and significance of differences was analyzed by Student's *t*-test. All results were derived from at least 3 independent experiments. Statistical significance was defined as $p < 0.05$.

Results

The expression profile of differential genes between NSCLC tissue samples with or without bone metastasis

In order to analyze the expression profile of genes in NSCLC with bone metastasis, microarray analysis was conduct on the NSCLC tissue samples with or without bone metastasis (n = 3). Firstly, principal components analysis (PCA) demonstrated an obvious segregation between non-metastatic and metastatic NSCLC tissue samples (Figure S1). Secondly, we adopted scatter plot to assess the overall distribution of data. The results also presented the distribution of the up-regulated (red), down-regulated (blue) and unchanged (gray) genes in (Fig. 1A). Next, Volcano plot was also applied to display the significant difference of genes between NSCLC tissue samples with or without bone metastasis (Fig. 1B). Through analysis, we discovered a total of 364 DEGs including 140 up-regulated genes and 224 down-regulated genes in NSCLC tissue samples with bone metastasis by using a cut-off value of fold change > 2.0 and $P < 0.05$. And the expression profile of the DEGs was demonstrated using the Heatmap (Fig. 1C). Besides, the detailed information of 140 up-regulated genes were presented in Table 2 (Fold-Change > 2, $P < 0.05$) and the detailed information of 224 down-regulated genes were presented in Table 3 (Fold-Change > 2, $P < 0.05$) .

GO and KEGG analyses of DEGs between NSCLC tissue samples with or without bone metastasis

In order to further obtain the critical annotation of DEGs, GO and KEGG analyses of the DEGs with a value more than 2-fold change were conducted in NSCLC tissue samples with bone metastasis. For the comparison of two NSCLC tissue samples with and without bone metastasis, the GO analysis of the upregulated genes was significantly enriched in 16 biological processes (BP), 13 cellular components (CC) and 6 molecular functions (MF). And the Top 3 BP included cellular process, metabolic process and

biological regulation; the Top3 CC included cell, cell part and organelle; the Top3 MF included binding, catalytic activity and structural molecule activity (Fig. 2A). Meanwhile, the GO analysis of the downregulated genes was significantly enriched in 17 BP, 8 CC and 6 MF. And the Top3 BP included cellular process, metabolic process and biological regulation; the Top3 CC included cell, cell part and organelle; the Top3 MF included binding, catalytic activity and nucleic acid binding transcription factor activity (Fig. 2B). Subsequently, the upregulated genes were mainly concentrated in the 5 pathways including cysteine and methionine metabolism, oxidative phosphorylation, parkinson disease, ribosome and thermogenesis (Fig. 2C); the downregulated genes were mainly concentrated in the transcriptional misregulation in cancer, ribosome, mitophagy-animal, bile secretion and apoptosis pathways (Fig. 2D).

COL6A1 was highly expressed in NSCLC tissue samples with bone metastasis

COL6A1, which is the most highly expressed gene in samples with bone metastasis compared to that without bone metastasis. As shown in Fig. 4A, the expression level of COL6A1 was significantly increased in samples with bone metastasis compared to that without bone metastasis. Consistent with this result, the IHC assay showed that increased expression of COL6A1 was also observed at the protein level (Fig. 4B), suggesting that COL6A1 might play an important role in the process of bone metastasis.

Identification of the osteogenetic ability

In order to do some preparation for bone metastasis tests, the osteogenetic abilities were investigated in HOB, hES-MP 002.5 and M-7 cells. We applied the osteoblast inducing conditional media to induce HOB, hES-MP 002.5 and M-7 cells for 14 days, respectively. The data of RT-qPCR assay exhibited that ALP and RUNX2 expressions were notably increased in induction group of HOB and hES-MP 002.5 cells compared to that in respective control group. while ALP and RUNX2 expressions did not change in M-7 cells after induction ($P < 0.001$, Fig. 5A). In addition, the results of Western blot also revealed that the levels of ALP and RUNX2 were higher in the osteogenic induced HOB and hES-MP 002.5 cells than the control cells, and ALP and RUNX2 expressions were low and did not change in M-7 cells (Fig. 5B).

Then, the degree of osteogenic differentiation was estimated in HOB, hES-MP 002.5 and M-7 cells. Firstly, Alizarin Red Staining was utilized to assess the calcium deposition of HOB, hES-MP 002.5 and M-7 cells. As demonstrated in Fig. 5C, HOB and hES-MP 002.5 cells showed weak osteoblasts under normal culture, and a large number of osteoblasts were observed after osteogenesis induction; no osteoblasts were presented in M-7 cells in normal culture, and few osteoblasts were found in M-7 cells after induction. Meanwhile, ALP staining was used to determine the ALP activity of HOB, hES-MP 002.5 and M-7 cells. We discovered that the ALP activity was dramatically enhanced in HOB and hES-MP 002.5 cells after osteogenic induction compared to that in normal cultured cells; After osteogenic induction, the ALP activity displayed a slight enhancement in M-7 cells (Fig. 5D).

COL6A1 promotes bone metastasis in vitro

Moreover, to investigate the impact of COL6A1 on osteogenic differentiation, we adopted HARA-B cells (lung cancer cells with strong bone metastases) to identify the effect of COL6A1 on cell adhesion. HOB,

hES-MP 002.5 and M-7 cells were co-cultured with HARA-B cells, which were stable expression of COL6A1 for 30 min. And the GFP-expressing cells were counted, the results demonstrated that overexpression of COL6A1 could memorably enhance the adhesion capacity of HARA-B cells after co-culture with HOB and hES-MP 002.5 cells, and knockdown of COL6A1 could dramatically attenuate the adhesion capacity of HARA-B cells after co-culture with HOB and hES-MP 002.5 cells. While COL6A1 did not change the adhesion capacity of HARA-B cells after co-culture with M-7 cells (Fig. 6).

Discussion

NSCLC is a frequent malignant tumor, and the morbidity and mortality are on the rise(16). Studies demonstrated that tumor stage, lymph node metastasis and bone metastasis are the main factors affecting the prognosis of NSCLC patients(17, 18). To further explore the gene markers and regulatory pathways related to bone metastasis in NSCLC, we applied the whole transcriptome expression microarray to compare the gene expression profiles between NSCLC tissue samples with and without bone metastasis. In our study, the bioinformatics data identified the key genes and pathways associated with the development of bone metastasis. By comparing gene expression differences between two groups of samples, we found 364 DEGs including 140 up-regulated genes and 224 down-regulated genes in NSCLC tissue samples with bone metastasis compared to that without bone metastasis.

GO and KEGG analysis are the crucial methods to predict and find target molecules and their regulatory networks related to disease occurrence(19–21). In order to quickly find the molecular regulatory network of DEGs related to the bone metastasis in NSCLC, GO and KEGG pathway enrichment analysis was performed to understand the biological functions of DEGs and functional pathways associated with bone metastasis. GO analysis denoted that the crucial biological processes of the DEGs in NSCLC tissue samples with bone metastasis were mainly associated with cellular process, metabolic process and biological regulation. And the binding and catalytic activity were also identified to be closely associated with the bone metastasis in NSCLC patients. Moreover, KEGG enrichment analysis displayed that the DEGs in NSCLC tissue samples with bone metastasis were mainly enriched in ribosome, apoptosis, cysteine and methionine metabolism, transcriptional misregulation in cancer, etc. Moreover, we disclosed that COL6A1, TST, APPL1, COA3 and TERF1 were prominently upregulated, and Prominin 2, RALY and CD133 were significantly downregulated in NSCLC tissue samples with bone metastasis. Among them, the expression difference of COL6A1 was the most significant in NSCLC tissue samples with bone metastasis.

COL6A1, which is located on chromosome 21, is a crucial gene belonging to the collagen family and studies have showed that it encodes the α1 (VI) chain of type VI collagen(22, 23). Type VI collagen is an extracellular matrix protein that plays crucial roles in maintaining the integrity of several tissues(24, 25). Studies have demonstrated that COL6A1 regulates functions of cell migration, differentiation and survival by participating in multiple signaling pathways such as apoptosis, proliferation, angiogenesis, fibrosis and inflammation(26). Its mutation has been demonstrated to be closely linked to many muscular-skeletal defects disorders such as Bethlam myopathy and Ulrich Congentical Muscular

Distrophy(27). Although COL6A1 is widely distributed in different tissues, its expression is markedly higher in pancreatic cancer tumor tissues with bone metastasis than that without bone metastasis(23). Thus, COL6A1 have demonstrated to be associated with the progression of many types of cancers(23, 28–31). For examples, a recent study reported that the mRNA expression and protein level of COL6A1 were increased in lung tissues of patients with pulmonary fibrosis, suggesting a strong association with between COL6A1 expression and NSCLC development. In addition, by utilizing quantitative secretome analysis, overexpression of COL6A1 was found to be increased in metastatic NSCLC cells, while COL6A1 suppression inhibited the metastatic activity of cancer cells. In a previous global secretome analysis of cell lines with varying bone metastatic ability from multiple cancer types, COL6A1 was identified as a new secreted mediator of bone metastasis. In our study, we further verified that COL6A1 could be significantly upregulated in NSCLC tissues with bone metastasis. Besides, we testified that COL6A1 also could dramatically induce the adhesion ability of HARA-B cells to osteoblasts. Therefore, we suggested that COL6A1 might be strongly associated with bone metastasis progression in NSCLC patients.

Conclusions

Based on the comprehensive whole transcriptome expression microarray analysis, the present study revealed a mass of crucial genes and pathways, which were associated with features of NSCLC with bone metastasis. Especially, COL6A1 was proven to induce the adhesion ability of HARA-B cells to osteoblasts. Therefore, we suggested that COL6A1 may become a novel therapeutic target for the treatment of advanced NSCLC patients with bone metastasis.

Abbreviations

NSCLC: non-small cell lung cancer

DEGs: DEGs

GO: Gene Ontology

KEGG: Kyoto Encyclopedia of Genes and Genomes

IPA: Ingenuity Pathway Analysis

COL6A1: collagen family collagen 6A1

SDS-PAGE: sodium dodecyl sulfate polyacrylamide gel electrophoresis

Declarations

Ethics approval and consent to participate:

The study protocol had been approved by the ethics committee of the Third Hospital of Hebei Medical University. All patients have signed the informed written consents.

Consent for publication:

Not applicable.

Availability of data and materials:

Not applicable.

Competing interests:

The authors declare that they have no competing interests.

Funding:

The present study was supported by the research project of training excellent clinical medical talents and basic research from Hebei Provincial Department of Finance and Hebei Provincial Health and Family Planning Commission (2017) (JCS [201746]). The funder Liu Ming conducted formal analysis , reviewed and edited the original draft.

Authors' contributions:

Data curation: NL, ZMZ

Formal analysis: NL, XHC, ML

Funding acquisition: ML

Investigation: NL, WL

Methodology: WL, YFL

Writing - original draft: NL, Writing - review & editing: ZMZ, ML

All authors read and approved the final manuscript.

Acknowledgements:

Not applicable.

References

1. Torre LA, Bray F, Siegel RL, Ferlay J, Lortet-Tieulent J, Jemal A. Global cancer statistics, 2012. CA Cancer J Clin. 2015;65(2).

2. Ferlay J, Colombet M, Soerjomataram I, Mathers C, Parkin DM, Pineros M, et al. Estimating the global cancer incidence and mortality in 2018: GLOBOCAN sources and methods. Int J Cancer. 2019;144(8).
3. Chen W, Zheng R, Baade PD, Zhang S, Zeng H, Bray F, et al. Cancer statistics in China, 2015. CA Cancer J Clin. 2016;66(2).
4. Ni Y, Ye X, Yang X, Huang G, Li W, Wang J, et al. Microwave ablation for non-small cell lung cancer with synchronous solitary extracranial metastasis. J Cancer Res Clin Oncol. 2020;146(5).
5. Nakahara Y, Hosomi Y, Shibuya M, Mitsufuji H, Katagiri M, Naoki K, et al. Multicenter study of zoledronic acid administration in non-small-cell lung cancer patients with bone metastasis: Thoracic Oncology Research Group (TORG) 1017. Mol Clin Oncol. 2019;11(4).
6. Oster G, Lamerato L, Glass AG, Richert-Boe KE, Lopez A, Chung K, et al. Natural history of skeletal-related events in patients with breast, lung, or prostate cancer and metastases to bone: a 15-year study in two large US health systems. Support Care Cancer. 2013;21(12).
7. Katakami N, Kunikane H, Takeda K, Takayama K, Sawa T, Saito H, et al. Prospective study on the incidence of bone metastasis (BM) and skeletal-related events (SREs) in patients (pts) with stage IIIB and IV lung cancer-CSP-HOR 13. J Thorac Oncol. 2014;9(2).
8. Zhang L, Gong Z. Clinical Characteristics and Prognostic Factors in Bone Metastases from Lung Cancer. Med Sci Monit. 2017;23.
9. Lang J, Zhao Q, He Y, Yu X. Bone turnover markers and novel biomarkers in lung cancer bone metastases. Biomarkers. 2018;23(6).
10. Pontarollo G, Confavreux CB, Pialat JB, Isaac S, Forest F, Yvorel V, et al. Bone decalcification to assess programmed cell death ligand 1 expression in bone metastases of non-small cell lung cancers. J Bone Oncol. 2020;21.
11. Ge L, Shao GR, Wang HJ, Song SL, Xin G, Wu M, et al. Integrated analysis of gene expression profile and genetic variations associated with ovarian cancer. Eur Rev Med Pharmacol Sci. 2015;19(14).
12. Shi WY, Liu KD, Xu SG, Zhang JT, Yu LL, Xu KQ, et al. Gene expression analysis of lung cancer. Eur Rev Med Pharmacol Sci. 2014;18(2).
13. Liao Y, Yin G, Wang X, Zhong P, Fan X, Huang C. Identification of candidate genes associated with the pathogenesis of small cell lung cancer via integrated bioinformatics analysis. Oncology letters. 2019;18(4).
14. Dennis G, Jr., Sherman BT, Hosack DA, Yang J, Gao W, Lane HC, et al. DAVID: Database for Annotation, Visualization, and Integrated Discovery. Genome Biol. 2003;4(5).
15. Zheng Y, Wang Q, Li T, Qian J, Lu Y, Li Y, et al. Role of Myeloma-Derived MIF in Myeloma Cell Adhesion to Bone Marrow and Chemotherapy Response. J Natl Cancer Inst. 2016;108(11).
16. Rotow J, Bivona TG. Understanding and targeting resistance mechanisms in NSCLC. Nature reviews Cancer. 2017;17(11).
17. Wang H, Zhang Y, Zhu H, Yu J. Risk factors for bone metastasis in completely resected non-small-cell lung cancer. Future oncology (London, England). 2017;13(8).

18. Yang XY, Liao JJ, Xue WR. FMNL1 down-regulation suppresses bone metastasis through reducing TGF-β1 expression in non-small cell lung cancer (NSCLC). Biomed Pharmacother. 2019;117.
19. Chen L, Zhang YH, Lu G, Huang T, Cai YD. Analysis of cancer-related lncRNAs using gene ontology and KEGG pathways. Artificial intelligence in medicine. 2017;76.
20. Ding J, Zhang Y. Analysis of key GO terms and KEGG pathways associated with carcinogenic chemicals. Combinatorial chemistry & high throughput screening. 2017.
21. Wang R, Yin C, Fu L, Liu J, Li J, Yin L. Expression profile analysis for epithelial-mesenchymal transition of breast cancer cell line DKTA based on microarray data. European Journal of Gynaecological Oncology. 2019;40(4).
22. Fujita A, Sato JR, Festa F, Gomes LR, Oba-Shinjo SM, Marie SK, et al. Identification of COL6A1 as a differentially expressed gene in human astrocytomas. Genet Mol Res. 2008;7(2).
23. Owusu-Ansah KG, Song G, Chen R, Edoo MIA, Li J, Chen B, et al. COL6A1 promotes metastasis and predicts poor prognosis in patients with pancreatic cancer. Int J Oncol. 2019;55(2).
24. Whittle MC, Izeradjene K, Rani PG, Feng L, Carlson MA, DelGiorno KE, et al. RUNX3 Controls a Metastatic Switch in Pancreatic Ductal Adenocarcinoma. Cell. 2015;161(6).
25. Zhu YP, Wan FN, Shen YJ, Wang HK, Zhang GM, Ye DW. Reactive stroma component COL6A1 is upregulated in castration-resistant prostate cancer and promotes tumor growth. Oncotarget. 2015;6(16).
26. Frka K, Facchinello N, Del Vecchio C, Carpi A, Curtarello M, Venerando R, et al. Lentiviral-mediated RNAi in vivo silencing of Col6a1, a gene with complex tissue specific expression pattern. J Biotechnol. 2009;141(1-2).
27. Llacua LA, Hoek A, de Haan BJ, de Vos P. Collagen type VI interaction improves human islet survival in immunoisolating microcapsules for treatment of diabetes. Islets. 2018;10(2).
28. Hou T, Tong C, Kazobinka G, Zhang W, Huang X, Huang Y, et al. Expression of COL6A1 predicts prognosis in cervical cancer patients. Am J Transl Res. 2016;8(6).
29. Lamandé SR, Bateman JF. Collagen VI disorders: Insights on form and function in the extracellular matrix and beyond. Matrix biology : journal of the International Society for Matrix Biology. 2018;71-72.
30. Sato T, Takano R, Tokunaka K, Saiga K, Tomura A, Sugihara H, et al. Type VI collagen α1 chain polypeptide in non-triple helical form is an alternative gene product of COL6A1. J Biochem. 2018;164(2).
31. Wan F, Wang H, Shen Y, Zhang H, Shi G, Zhu Y, et al. Upregulation of COL6A1 is predictive of poor prognosis in clear cell renal cell carcinoma patients. Oncotarget. 2015;6(29).

Tables

Due to technical limitations, table 2 & 3 xlsx are only available as a download in the Supplemental Files section.

Figures

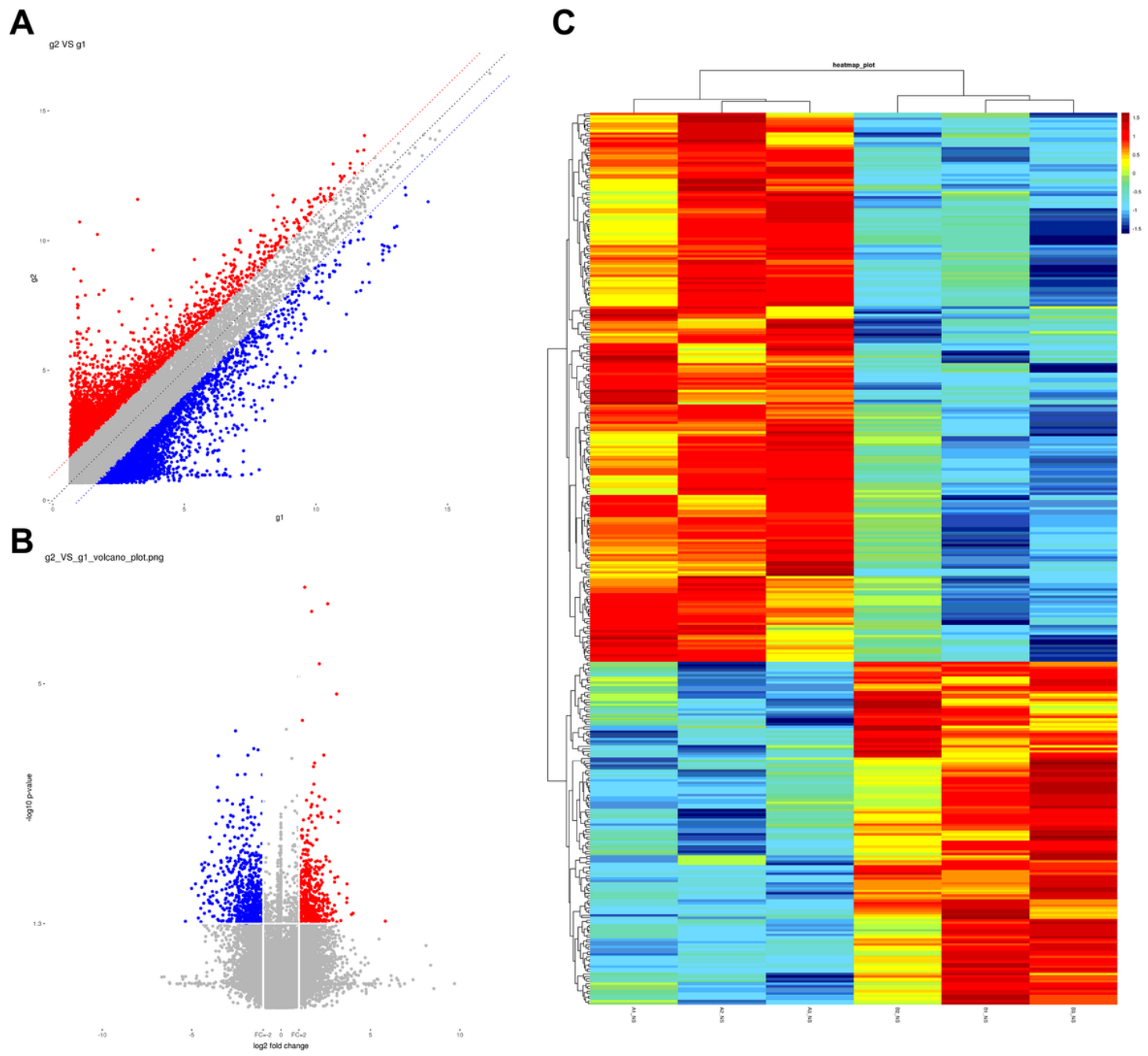

Figure 1

The expression profile of differential genes between NSCLC tissue samples with or without bone metastasis. (A) Scatter plot was applied to evaluate the overall distribution of two sets of data. Red represents the upregulated genes, and blue represents the downregulated genes. (B) Volcano plot was utilized to display the significant difference of genes between NSCLC tissue samples with or without bone metastasis. (C) Heatmap was adopted to show the expression profile of the DEGs.

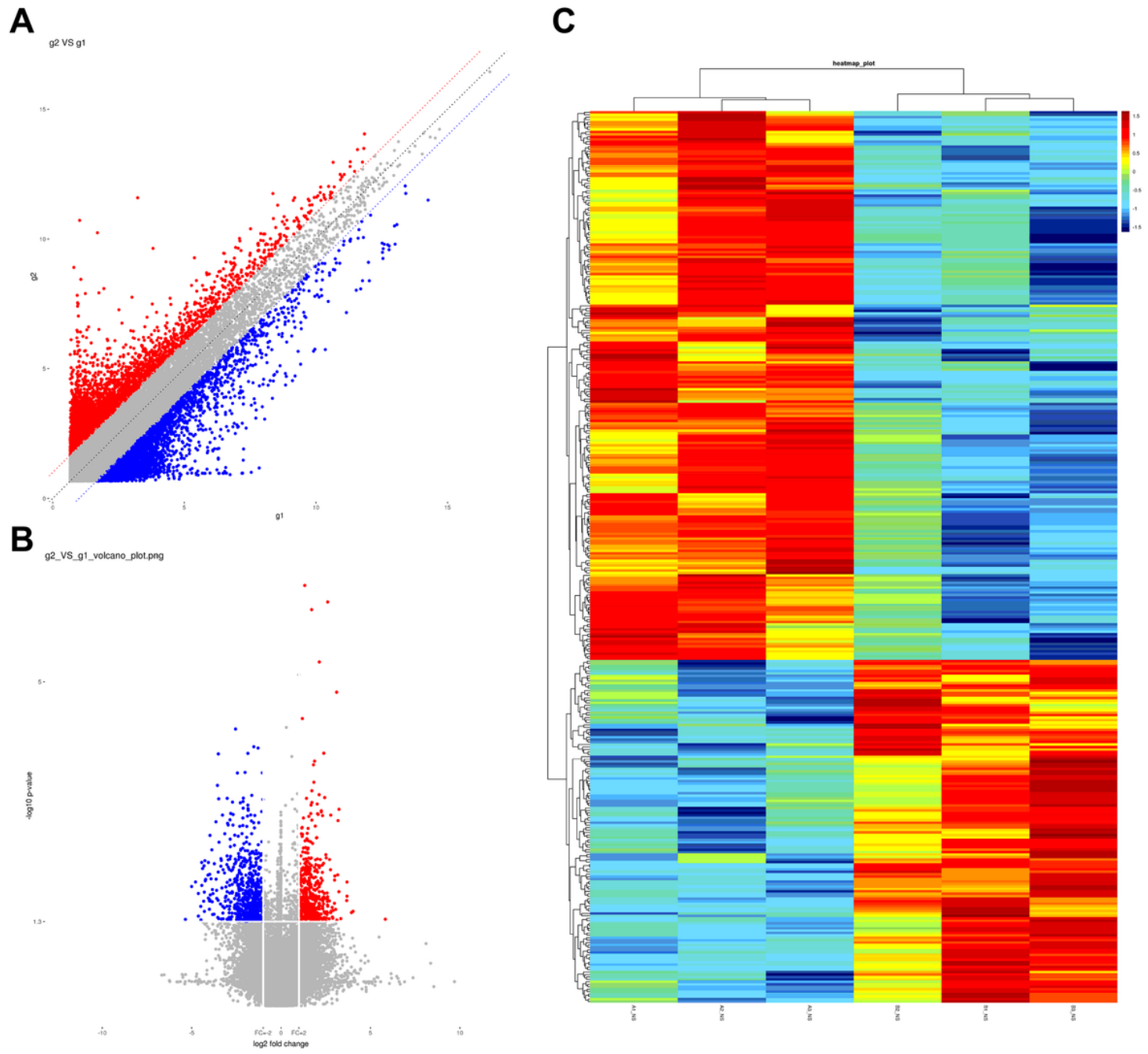

Figure 1

The expression profile of differential genes between NSCLC tissue samples with or without bone metastasis. (A) Scatter plot was applied to evaluate the overall distribution of two sets of data. Red represents the upregulated genes, and blue represents the downregulated genes. (B) Volcano plot was utilized to display the significant difference of genes between NSCLC tissue samples with or without bone metastasis. (C) Heatmap was adopted to show the expression profile of the DEGs.

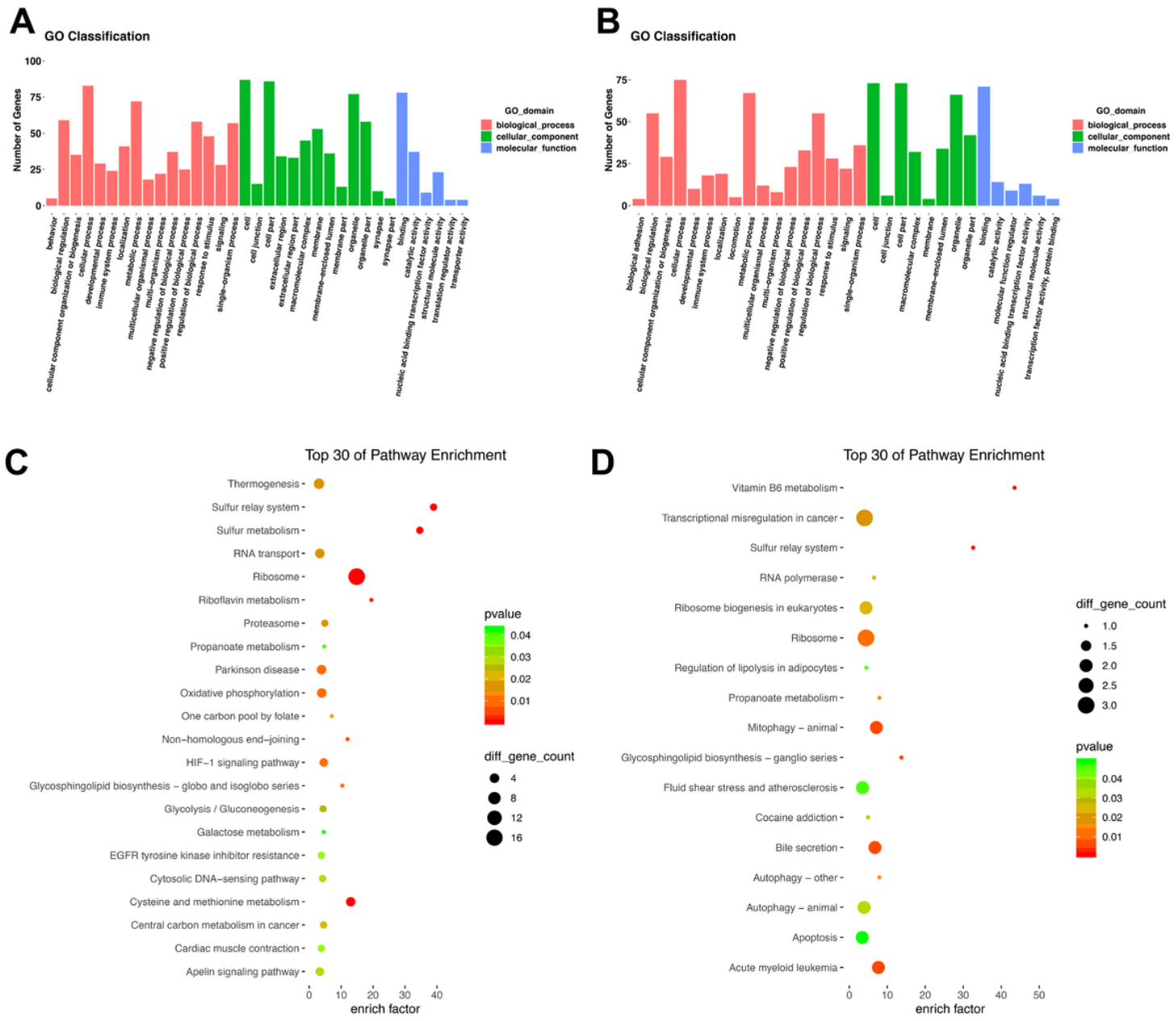

Figure 2

GO and KEGG analyses of DEGs. (A) The GO analysis of the upregulated genes in NSCLC tissues with bone metastasis. (B) The GO analysis of the downregulated genes in NSCLC tissues with bone metastasis. (C) The KEGG analysis of the upregulated genes in NSCLC tissues with bone metastasis. (D) The KEGG analysis of the downregulated genes in NSCLC tissues with bone metastasis.

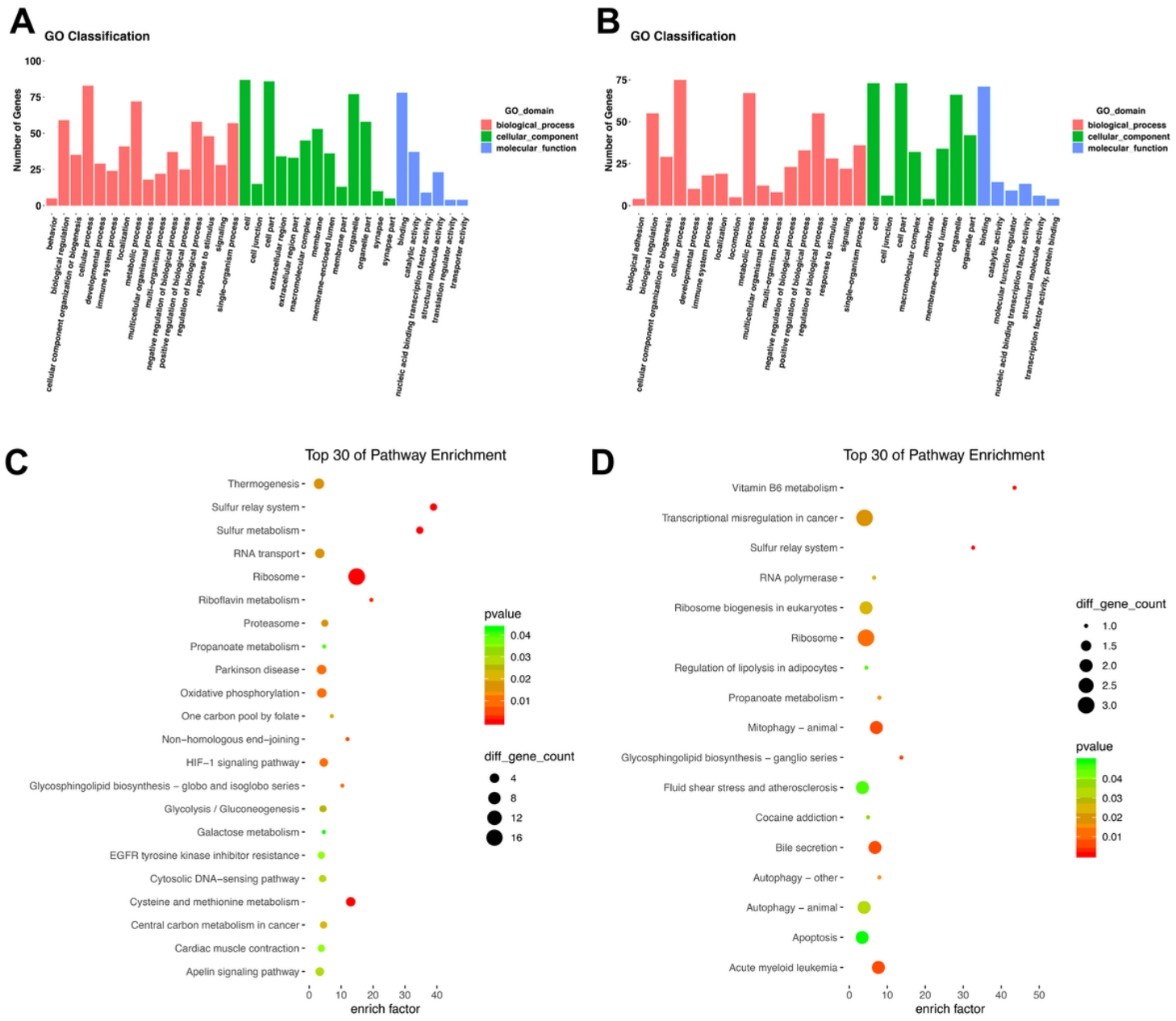

Figure 2

GO and KEGG analyses of DEGs. (A) The GO analysis of the upregulated genes in NSCLC tissues with bone metastasis. (B) The GO analysis of the downregulated genes in NSCLC tissues with bone metastasis. (C) The KEGG analysis of the upregulated genes in NSCLC tissues with bone metastasis. (D) The KEGG analysis of the downregulated genes in NSCLC tissues with bone metastasis.

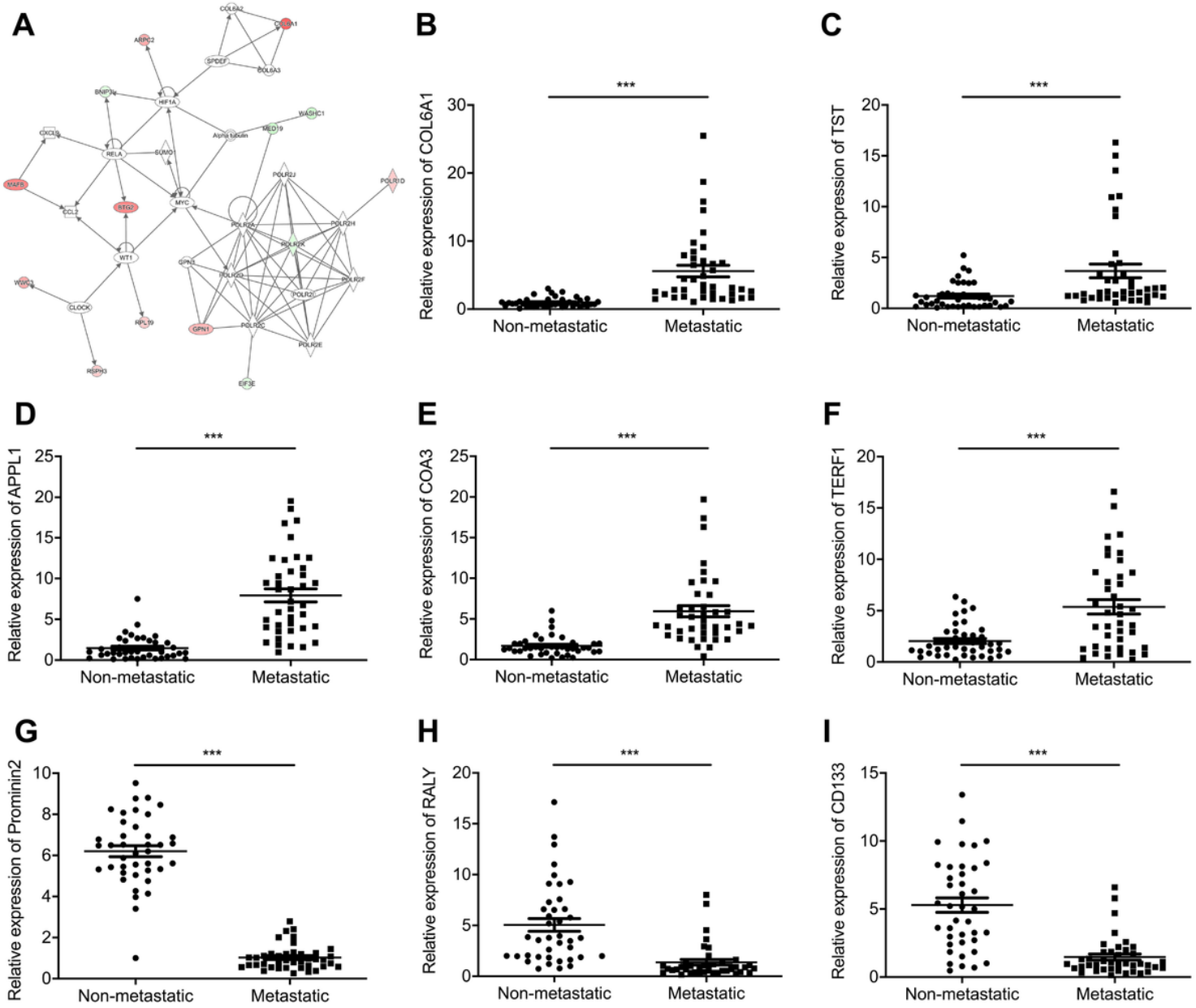

Figure 3

Network analysis by the Ingenuity Pathway Analysis (IPA) and identification of 8 genes. (A) Top networks of genes were displayed using the IPA in NSCLC tissue samples with bone metastasis. RT-qPCR analysis was conducted to confirm the expressions of COL6A1 (B), TST (C), APPL1 (D), COA3 (E), TERF1 (F), Prominin 2 (G), RALY (H) and CD133 (I) in NSCLC tissue samples with or without bone metastasis, ***P<0.001.

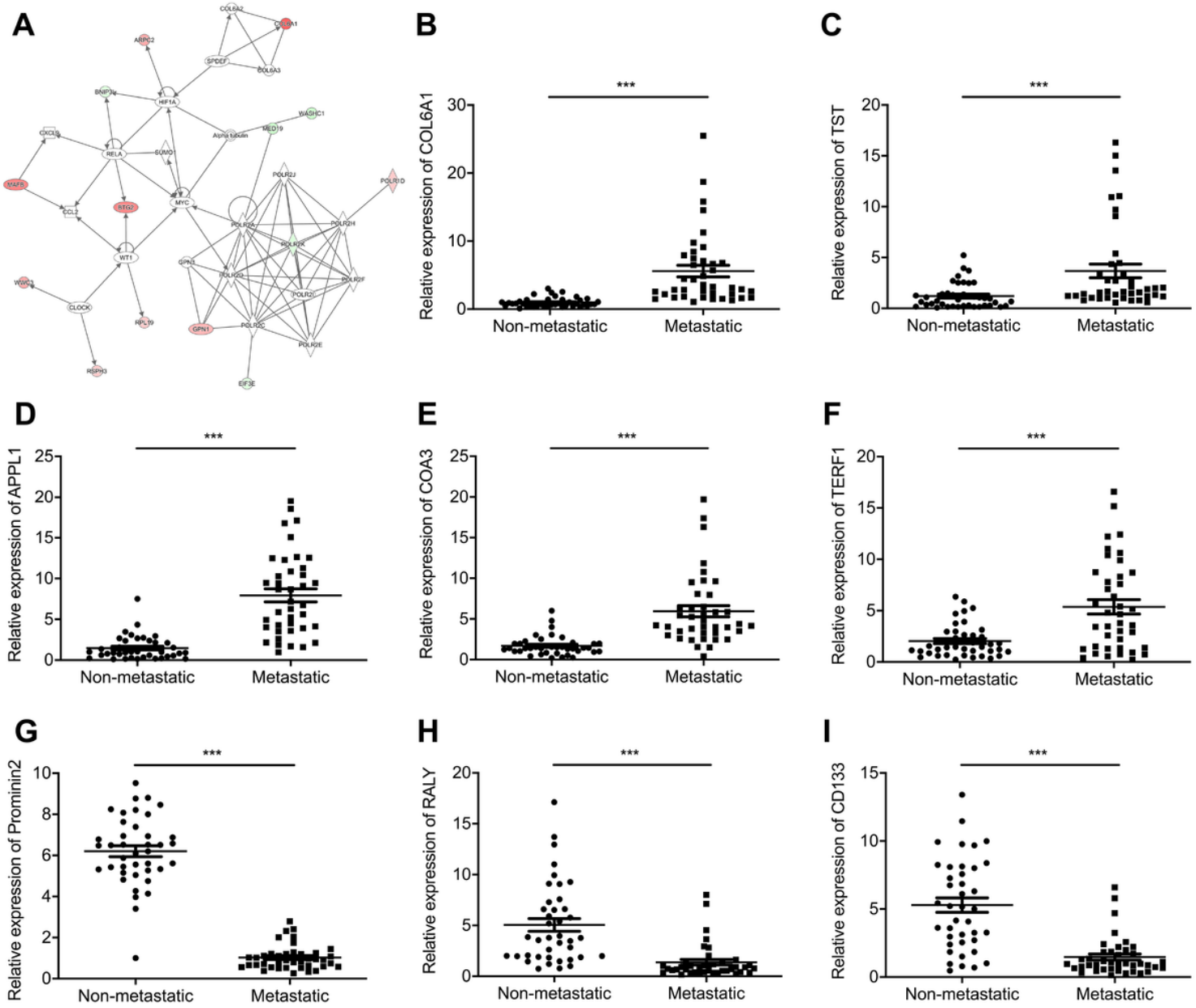

Figure 3

Network analysis by the Ingenuity Pathway Analysis (IPA) and identification of 8 genes. (A) Top networks of genes were displayed using the IPA in NSCLC tissue samples with bone metastasis. RT-qPCR analysis was conducted to confirm the expressions of COL6A1 (B), TST (C), APPL1 (D), COA3 (E), TERF1 (F), Prominin 2 (G), RALY (H) and CD133 (I) in NSCLC tissue samples with or without bone metastasis, ***P<0.001.

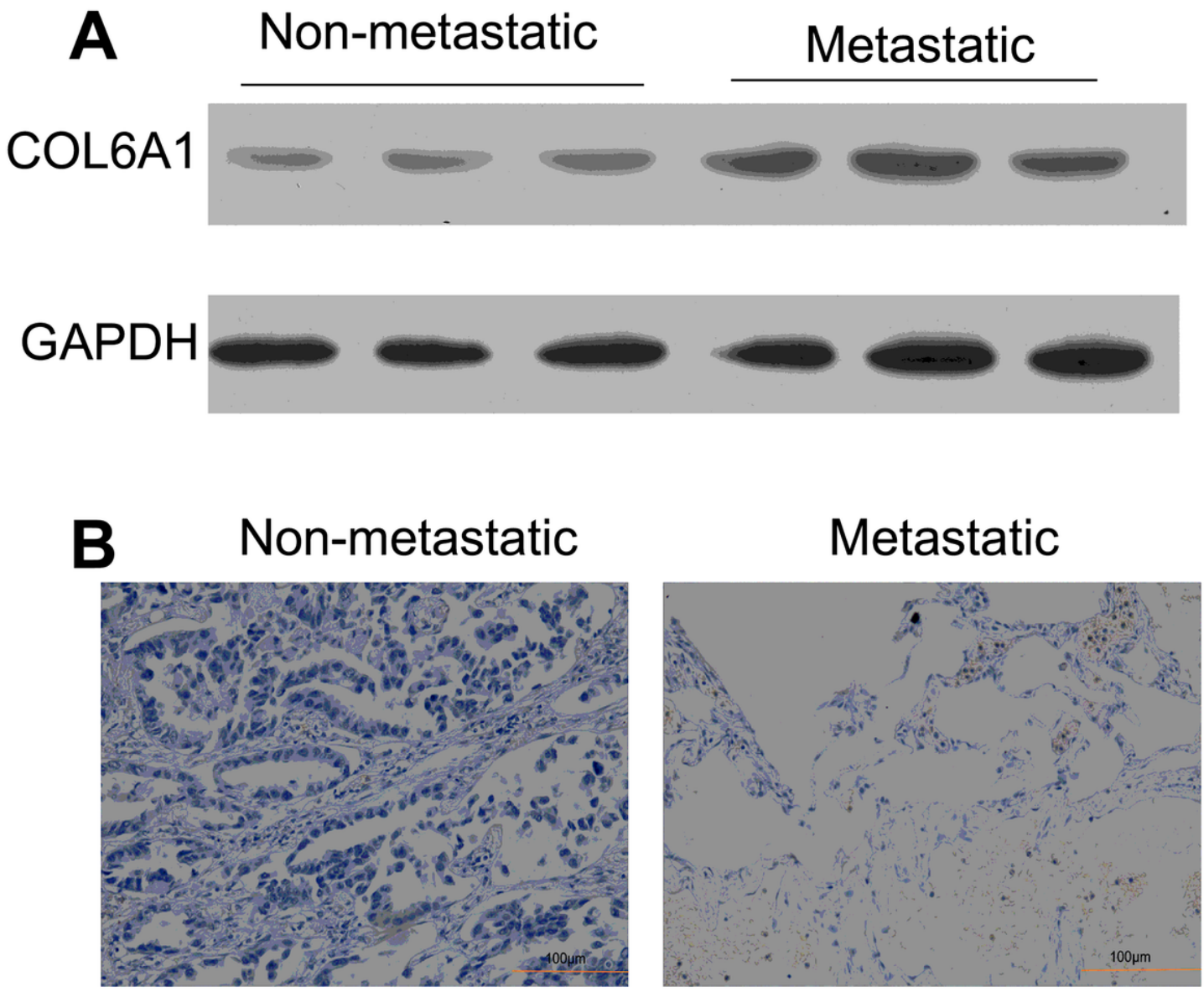

Figure 4

COL6A1 was highly expressed in NSCLC tissue samples with bone metastasis. (A) COL6A1 expression was determined by western blotting analysis. (B) IHC assay was adopted to assess the COL6A1 expression NSCLC tissue samples with and without bone metastasis. Magnification, ×100; Scale bar=100μm.

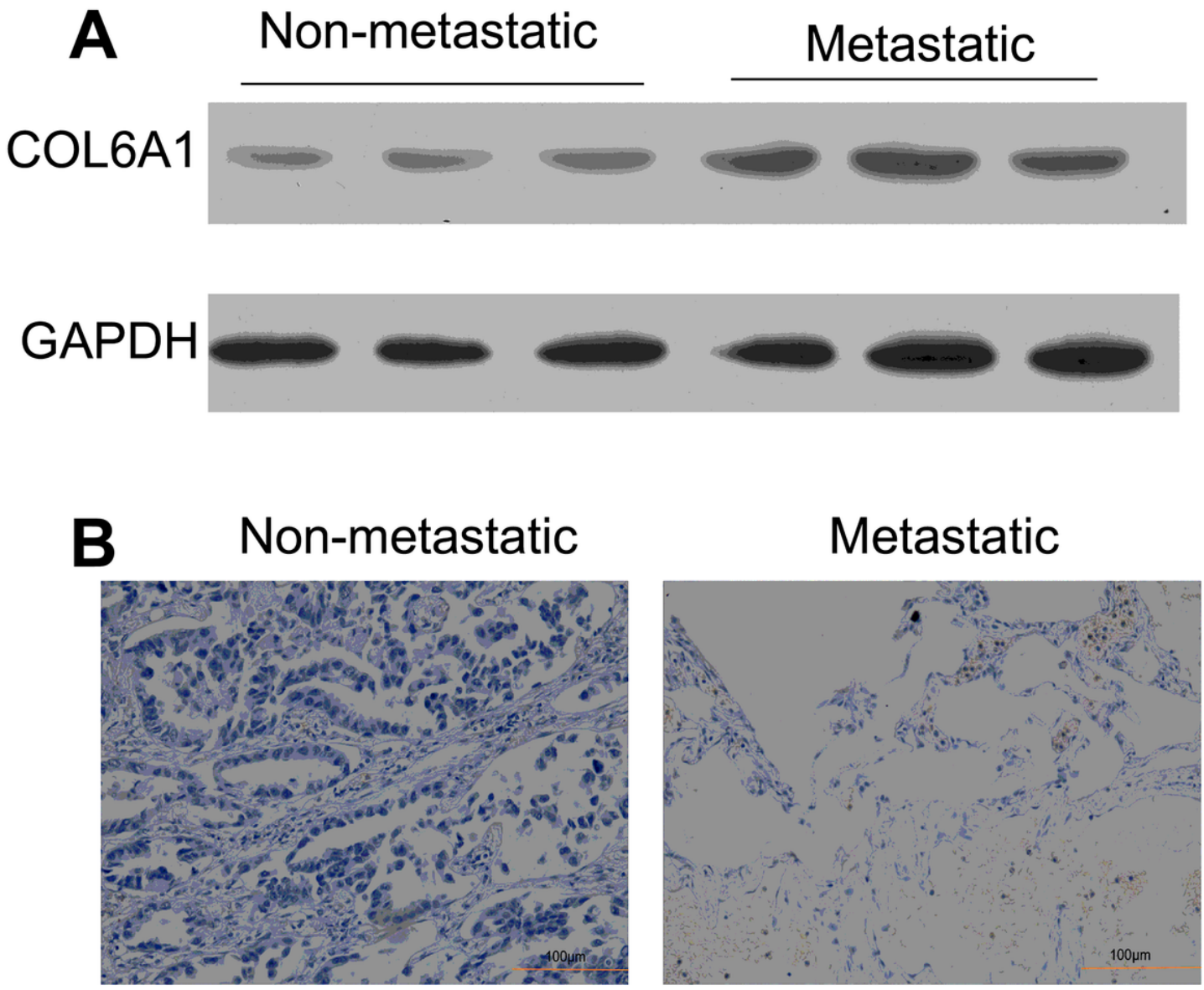

Figure 4

COL6A1 was highly expressed in NSCLC tissue samples with bone metastasis. (A) COL6A1 expression was determined by western blotting analysis. (B) IHC assay was adopted to assess the COL6A1 expression NSCLC tissue samples with and without bone metastasis. Magnification, ×100; Scale bar=100μm.

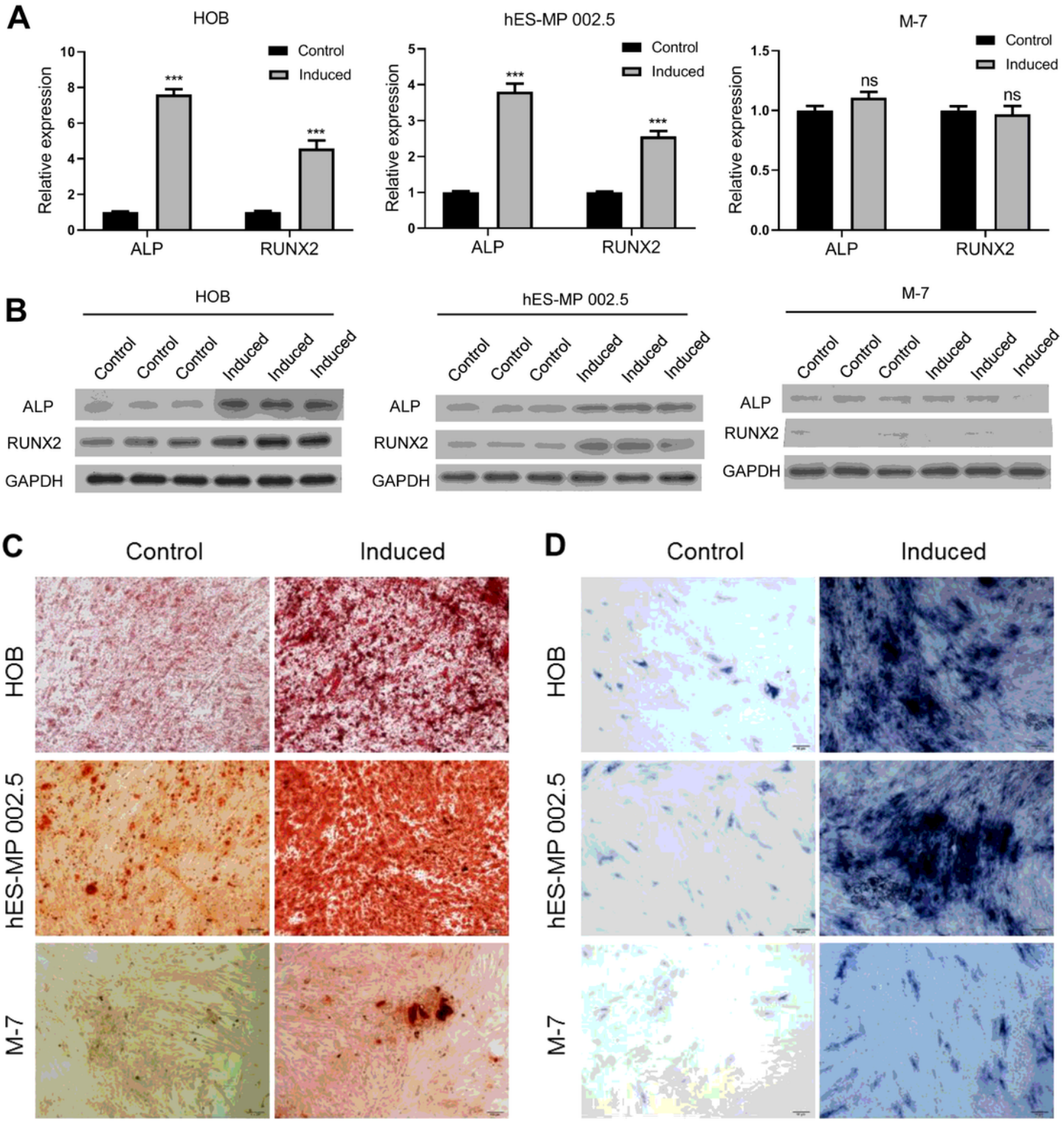

Figure 5

Induction and identification of osteoblasts. HOB, hES-MP 002.5 and M-7 were induced using the osteoblast inducing conditional media for 14 days, respectively. (A) RT-qPCR and (B) Western blot assays were conducted to analyze the expressions of ALP and RUNX2 in osteoblast induced and non-induced cells. (C) The calcium deposition was examined using Alizarin Red Staining in HOB, hES-MP 002.5 and M-7 cells after osteogenic induction. Magnification, ×100; Scale bar=100μm. (D) The ALP activity was

determined by ALP staining in the induced and uninduced HOB, hES-MP 002.5 and M-7 cells. Magnification, ×100; Scale bar=100μm. ***P<0.001.

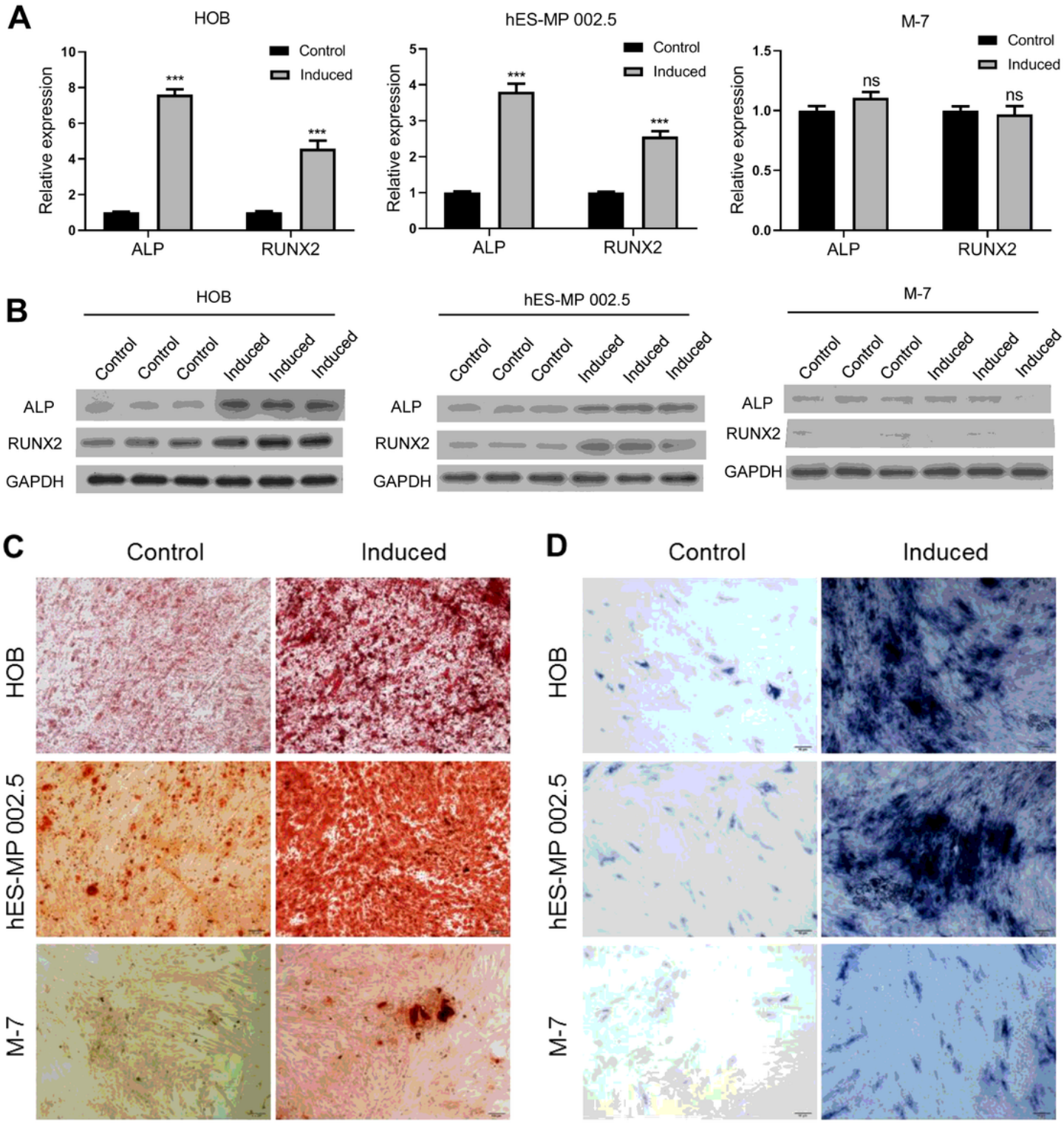

Figure 5

Induction and identification of osteoblasts. HOB, hES-MP 002.5 and M-7 were induced using the osteoblast inducing conditional media for 14 days, respectively. (A) RT-qPCR and (B) Western blot assays were conducted to analyze the expressions of ALP and RUNX2 in osteoblast induced and non-induced

cells. (C) The calcium deposition was examined using Alizarin Red Staining in HOB, hES-MP 002.5 and M-7 cells after osteogenic induction. Magnification, ×100; Scale bar=100μm. (D) The ALP activity was determined by ALP staining in the induced and uninduced HOB, hES-MP 002.5 and M-7 cells. Magnification, ×100; Scale bar=100μm. ***P<0.001.

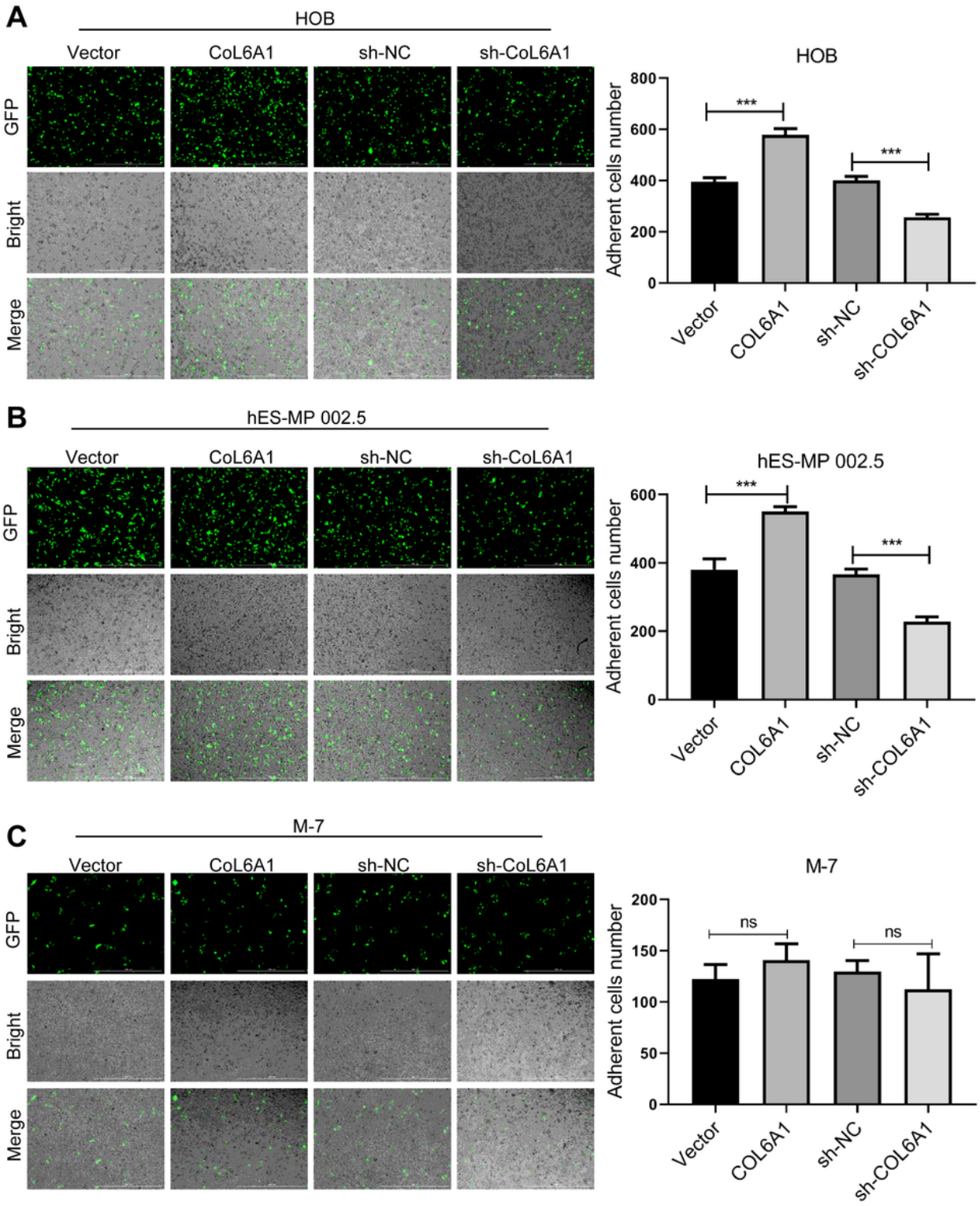

Figure 6

COL6A1 induced the adhesion ability of HARA-B cells after co-culture with HOB, hES-MP 002.5 cells. HARA-B cells were transfected with COL6A1 overexpressed plasmid, COL6A1 shRNAs and respective control plasmids, respectively. The adhesion capacity of HARA-B cells in each group were checked by applying the adhesion experiment after co-culture with HOB (A), hES-MP 002.5 (B) and M-7 cells (C) for 30 min. Magnification, ×100; Scale bar=100μm.

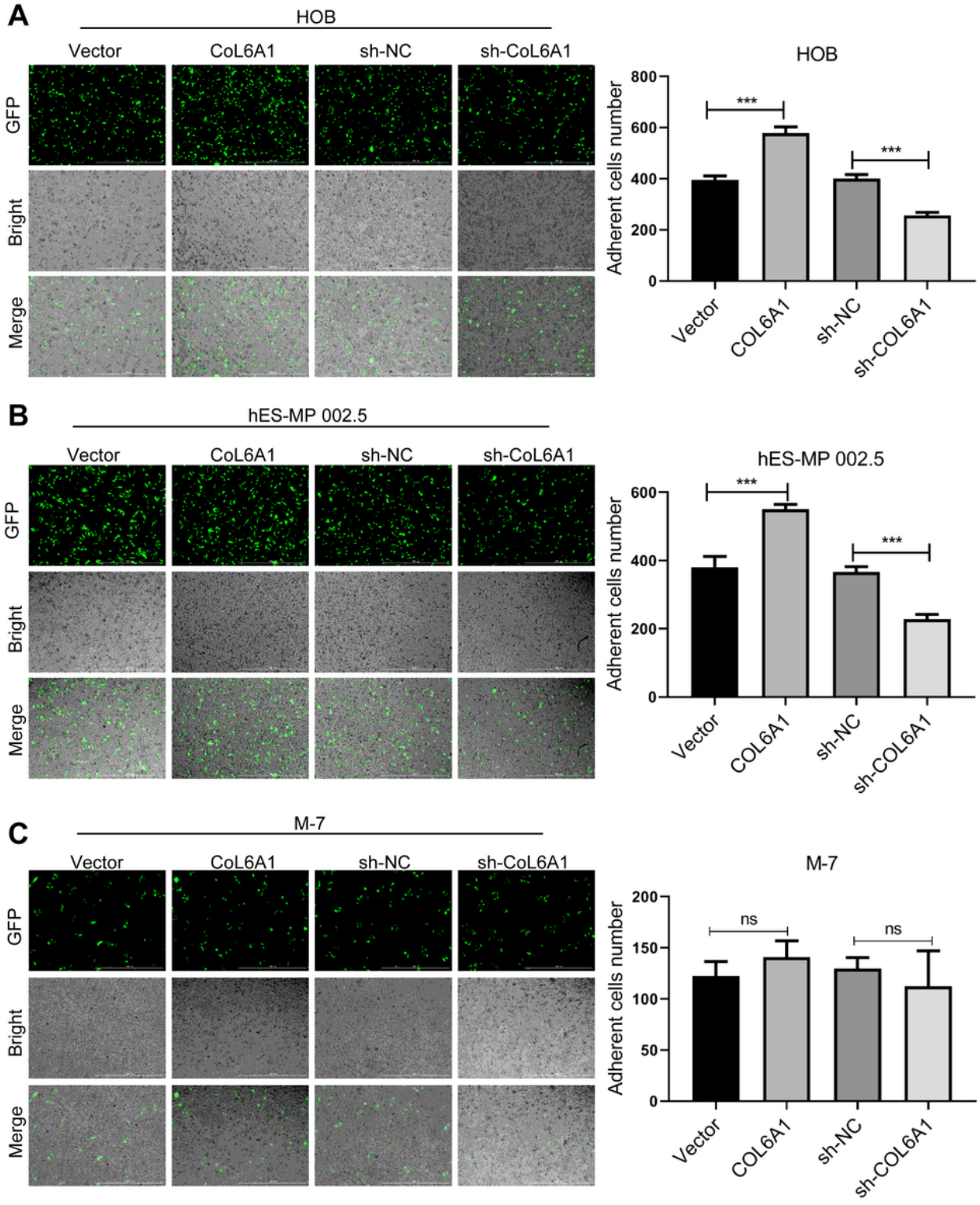

Figure 6

COL6A1 induced the adhesion ability of HARA-B cells after co-culture with HOB, hES-MP 002.5 cells. HARA-B cells were transfected with COL6A1 overexpressed plasmid, COL6A1 shRNAs and respective control plasmids, respectively. The adhesion capacity of HARA-B cells in each group were checked by applying the adhesion experiment after co-culture with HOB (A), hES-MP 002.5 (B) and M-7 cells (C) for 30 min. Magnification, ×100; Scale bar=100μm.

Supplementary Files

This is a list of supplementary files associated with this preprint. Click to download.

- Table2upregulatedgenes.xlsx
- Table2upregulatedgenes.xlsx
- Table3downregulatedgenes.xlsx
- Table3downregulatedgenes.xlsx
- Supplementarymaterials.docx
- Supplementarymaterials.docx
- FigureS1.tif
- FigureS1.tif